ACS APPLIED MATERIALS & INTERFACES

www.acsami.org

Research Article

Role of Environment on the Shear-Induced Structural Evolution of MoS_2 and Impact on Oxidation and Tribological Properties for Space Applications

Tomas F. Babuska, John F. Curry, Michael T. Dugger, Ping Lu, Yan Xin, Sam Klueter, Alexander C. Kozen, Tomas Grejtak, and Brandon A. Krick*

Cite This: *ACS Appl. Mater. Interfaces* 2022, 14, 13914–13924

Read Online

ACCESS | Metrics & More | Article Recommendations

ABSTRACT: This work investigates the role of water and oxygen on the shear-induced structural modifications of molybdenum disulfide (MoS_2) coatings for space applications and the impact on friction due to oxidation from aging. We observed from transmission electron microscopy (TEM) and X-ray photoelectron spectroscopy (XPS) that sliding in both an inert environment (i.e., dry N_2) or humid lab air forms basally oriented (002) running films of varying thickness and structure. Tribological testing of the basally oriented surfaces created in dry N_2 and air showed lower initial friction than a coating with an amorphous or nanocrystalline microstructure. Aging of coatings with basally oriented surfaces was performed by heating samples at 250 °C for 24 h. Post aging tribological testing of the as-deposited coating showed increased initial friction and a longer transition from higher friction to lower friction (i.e., run-in) due to oxidation of the surface. Tribological testing of raster patches formed in dry N_2 and air both showed an improved resistance to oxidation and reduced initial friction after aging. The results from this study have implications for the use of MoS_2-coated mechanisms in aerospace and space applications and highlight the importance of preflight testing. Preflight cycling of components in inert or air environments provides an oriented surface microstructure with fewer interaction sites for oxidation and a lower shear strength, reducing the initial friction coefficient and oxidation due to aging or exposure to reactive species (i.e., atomic oxygen).

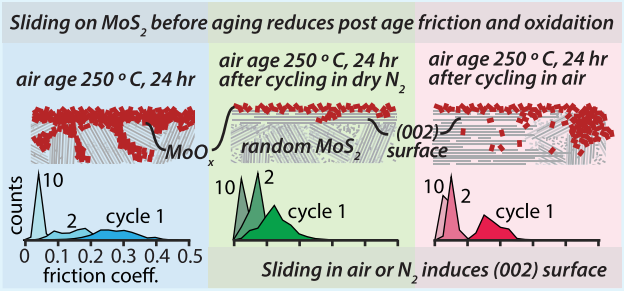

KEYWORDS: *MoS_2, aging, oxidation, friction, wear, environment*

1. INTRODUCTION

Components coated with molybdenum disulfide (MoS_2) to be used in space are likely tested in a lab environment prior to storage and launch to ensure mechanism functionality.[1] Testing is commonly done in a climate-controlled assembly facility or with controlled humidity; critical systems can be tested in thermal vacuum chambers. Additionally, many assemblies undergo vibration and thermal preflight qualification. Slip and microslip events caused during activities ranging from preflight component testing to vibration testing could alter the surface microstructure of MoS_2-based materials. Here, we study how this surface microstructure will influence oxidation resistance and friction evolution during initial sliding ("run-in") cycles. This is critical to common applications of MoS_2 coatings in single and low-cycle systems that need to actuate or slide just once at deployment or a few times while in space. As such, the initial friction on orbit after preflight sliding, aging in terrestrial air, and atomic oxygen exposure as it passes through low earth orbit can be critical to mission success.

MoS_2 coatings are used as solid lubricants for aerospace components due to the material's extremely low coefficient of friction in vacuum and inert environments (<0.05).[1−3] The transition from initially higher friction to low friction (run-in) is a result of a two-step process: shear inducing a reorientation and coalescence of MoS_2 lamella to a basal orientation (i.e., formation of a tribofilm) and the formation of a transfer film.[4−8] The low coefficient of friction is a result of the basally oriented lamellae have a low shear strength due to weak van der Waals interactions between sulfur-terminated basal planes.[9,10] Though the tribological properties of MoS_2 solid lubricants are superior in vacuum or inert environments, MoS_2 is highly sensitive to water and oxygen contamination which

Received: December 24, 2021
Accepted: February 24, 2022
Published: March 10, 2022

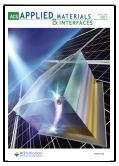

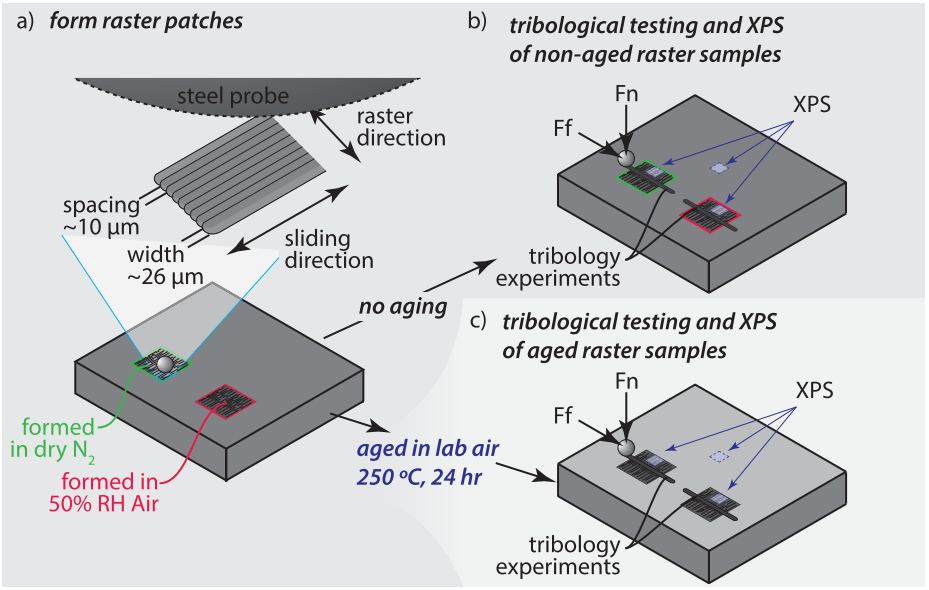

Figure 1. (a) Schematic showing the process of creating raster patches in lab air and dry N_2. (b) Tribological testing and XPS of the different raster patches without any aging and (c) with aging at 250 °C for 24 h.

can cause high friction (~0.2) and premature component failure due to high friction and wear.[11−13] Coating microstructure can change the tribological properties of MoS_2 in the presence of water and oxygen.[14−19] Additives such as Ti, Ni, Au, Sb_2O_3, and C have been added to coatings and have demonstrated improved wear life and friction when tested in humid air environments.[20−26]

Mechanical impingement of pure MoS_2 particles in a nitrogen gas stream results in basally oriented coatings that exhibit lower initial friction and faster run-in to low friction in inert environments than randomly oriented sputtered coatings.[27] This occurs because the large basally oriented crystallites of the nitrogen-sprayed films do not have to reorient during the first few cycles of sliding.[27] The impingement MoS_2 coatings also had a friction coefficient ~2× lower than sputtered MoS_2 coatings in humid air.[27] This is a result of their basal orientation, where low shear strength interfaces between lamella are parallel to the sliding direction. In contrast, randomly oriented sputtered coatings must be run-in to form a basally oriented surface that yields low friction. In air, water vapor and oxygen inhibit growth and reorientation of these surface running films, preventing low friction performance.[28]

Water and oxygen not only affect the tribological properties in dynamic sliding but also can adversely affect a coating during passive exposure for prolonged periods of time, or aging, that can lead to oxidation.[29−32] Prolonged storage has been shown to significantly degrade the performance of MoS_2 coatings; Lince et al. exposed MoS_2 for up to four years in humid lab air conditions and found that the cycles to failure decreased by as much as 80%.[30] Aging studies of MoS_2 have been mostly limited to as-deposited coatings. Coatings without any sliding history exhibit more susceptibility to oxidation due to nanocrystalline microstructures having more available edge sites for interactions with environmental contaminants.[29] Curry et al. performed accelerated aging experiments (250 °C O_2 at atmospheric pressure for 30 min) on basally oriented and nanocrystalline coatings and found that a basally oriented microstructure limits the amount of surface oxidation and prevents oxygen from penetrating the coating;[29] additionally, they reported the basally oriented films have lower initial friction and faster transition to steady state than nanocrystalline films before and after aging.

Relationships between the running films formed during preflight run-in, oxidative aging, and the tribological performance in the operating environment must be understood to enable optimum application of these materials. The evolution of the surface microstructure due to sliding is known, yet the impact that water and oxygen have on structurally altering the surface under shear is not well understood. This work aims to better understand how sliding changes the surface microstructure of MoS_2 coatings in the presence of water and oxygen and the impact of shear-induced changes on the tribological properties before and after aging. To do this, we form large area running films in different environments by rastering a microtribometer (comparable experiments with atomic force microscopes[33]). The tribological properties of the run-in films are studied before and after accelerated aging.

2. EXPERIMENTAL SECTION

2.1. Materials Synthesis. Pure MoS_2 coatings (~1 μm thick) were deposited on polished 440C steel substrates (~20 nm average roughness) via DC magnetron sputtering by using 1.5 mTorr of Ar and a 3 in. MoS_2 target at 150 W and 30 V bias for 30 min (Tribologix Inc., Golden, CO). A 10 nm Cr adhesion layer was initially deposited on the substrates by using arc evaporation. Samples were annealed prior to tribological testing at 150 °C for 24 h in a vacuum oven (100 kPa vacuum) to drive off latent water and contaminants from the coating and subsequently stored in a vacuum desiccator between tests to prevent degradation.

2.2. Tribological Test Methods. *2.2.1. Raster Method and Accelerated Aging.* Large regions of sheared MoS_2 were required to permit surface analysis via X-ray photoelectron spectroscopy (XPS) of the mechanically reoriented material. So-called "raster patches" were formed by overlapping multiple small parallel sheared regions (wear scars) (Figure 1a). Wear scars were formed by using a microtribometer[34−36] in lab air (~50% RH ± 5%) and dry N_2 (O_2 < 0.5 ppm, H_2O < 0.5 ppm) to compare the effects of run-in environment. The counterface was a 3 mm diameter 440C stainless steel ball (new ball for each patch) at a load of 200 mN, resulting in a maximum

https://doi.org/10.1021/acsami.1c24931
ACS Appl. Mater. Interfaces 2022, 14, 13914−13924

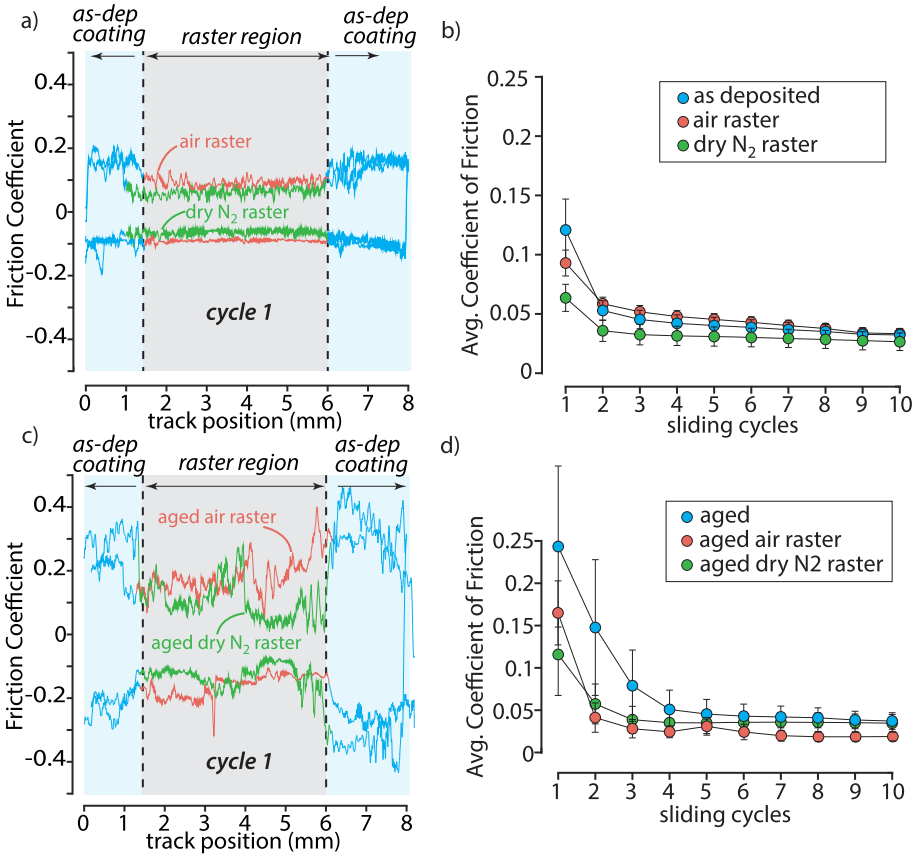

Figure 2. (a) Cycle 1 data of friction coefficient vs track position for the air raster and dry N_2 raster before aging with corresponding as-deposited and raster regions where average data points were taken. (b) Average coefficient of friction values for the as-deposited, air raster, and dry N_2 raster regions over the first 10 sliding cycles before aging. (c) Cycle 1 friction loop after accelerated aging with the corresponding as-deposited and raster regions where averages where calculated. (d) Average coefficient of friction values for aged as-deposited, air raster, and dry N_2 raster region for the first 10 sliding cycles.

Hertzian contact pressure of ~600 MPa and elastic contact width of ~25 μm. Each individual wear scar was slid for 5 mm and 20 bidirectional reciprocating sliding cycles (steady state was achieved after 20 cycles). After 20 cycles the sample was moved 10 μm (60% of the Hertzian contact width) using a stepper stage, and 20 more cycles of sliding were performed as a new wear scar. This was continued for 500 raster lines (10000 total sliding cycles), resulting in 5 × 5 mm^2 of mechanically reoriented material.

Raster patches were formed on separate samples in dry nitrogen and in 50% RH air. Selected samples were subsequently subjected to an accelerated aging treatment consisting of heating in an oven to 250 °C air for 24 h.

2.2.2. Tribological Measurement and Metric. After the raster patches were created in either lab air or dry N_2 and aged (where applicable), the friction inside and outside of the raster patch was tested in dry N_2 (O_2 < 0.5 ppm, H_2O < 0.5 ppm) with a new 3 mm diameter 440C ball at 200 mN. The ball was slid in a reciprocating bidirectional fashion perpendicularly across each region at a sliding velocity of 2 mm/s, starting in the as-deposited region on one side of the raster patch and ending on the opposite side before returning for both the nonaged sample (Figure 1a) and aged sample (Figure 1c). Friction loops (Figure 1a,c) show the position resolved coefficient of friction of a complete reciprocating sliding cycle (a positive force is observed on the forward stroke and a negative force on the reverse stroke) and is used to calculate average coefficient of friction and account for sensor offsets or misalignments.[36] The cycle-average coefficient of friction and standard deviation was calculated for the unworn regions of each sample to the sides of each raster patch by pooling the position resolved friction loop data outside the raster patch (Figure 2a, blue region) and, similarly, for the raster region by pooling the friction loop data inside the raster patch (Figure 2a, gray region).

The position resolved friction loop data were acquired at 1 kHz allowing for histograms showing the distribution of the friction coefficient within a cycle to be plotted (Figure 6b,d,h,j,l,n). For example, the histogram of cycle 1 shown in Figure 6b is of all the data from the blue region of Figure 2a. Similarly, the histograms of cycle 1 shown in Figure 6h,l is the data in the gray region of Figure 2a plotted as a distribution of friction coefficient.

2.3. X-ray Photoelectron Spectroscopy (XPS). XPS was measured in the as-deposited, air raster, and dry N_2 regions to characterize the chemical composition of each surface and the effects of shearing in different environments has on the MoS_2 chemistry. XPS was performed in three different regions after aging—in the as-deposited, air raster, and dry N_2 raster—to understand the effect of surface treatment on oxidation resistance.

XPS was performed by using a Kratos Ultra DLD XPS system using a 12 kV monochromatic Al Kα X-ray source (1486.7 eV) in hybrid lens mode with charge neutralization. Survey spectra were collected with a step size of 1 eV and pass energy of 160 eV. High-resolution spectra were collected with a step size of 0.1 eV and pass energy of 20 eV. Sputtering was performed by using 5 kV Ar^+ ion beam with a 3 × 3 mm^2 raster area for 10 min. XPS data were analyzed by using CasaXPS with peak area quantification normalized by standard photoionization cross sections corrected for the instrument geometry and a Shirley background algorithm.

2.4. Focused Ion Beam (FIB) Sample Preparation and Transmission Electron Microscopy (TEM). FIB cross sections of as-deposited and sheared MoS_2 regions were prepared for TEM analysis. Cross sections were prepared perpendicular to regions slid in lab air and dry N_2 so that half of the section was sheared MoS_2 and

https://doi.org/10.1021/acsami.1c24931
ACS Appl. Mater. Interfaces 2022, 14, 13914−13924

half was the as-deposited coating. This was performed to ensure that the FIB did not modify the surface of the coating. FIB cross sections had a 2 μm thick protective Pt layer deposited by first the electron beam and then the ion beam. A 21 nA ion beam was used to cut trenches on both sides of the Pt layer. The protected section was then thinned to 250 nm with 0.3 nA ion beam. The cross section was welded to the needle and extracted from the sample. The lamella was then attached to the copper grid and thinned to <100 nm with decreasing bean current. The final polishing step was done with 0.3 nA and 3 kV ion beam. The lamella was studied with the TEM at 200 kV (JEOL JEM-ARM200cF, Tokyo, Japan). The TEM images were acquired with a Gatan Ultrascan CCD camera. Scanning TEM (STEM) images, both dark-field and bright-field STEM images, were acquired with a probe size of 0.078 nm. The images were processed and analyzed in DigitalMicrograph (Gatan, Pleasaton, CA).

A second set of FIB cross sections were taken on a separate wear scar that was slid in lab air at Sandia National Laboratories. Two cross sections were taken perpendicular to the wear scar, and a separate cross section was taken in an as-deposited region. The structural analyses for these samples were performed by using an aberration-corrected scanning TEM (FEI Titan G2 80-200 STEM) operated at 200 kV. *Z*-contrast or high-angle annular dark-field (HAADF) imaging was used for the structural analysis.

3. RESULTS AND DISCUSSION

3.1. Shear-Induced Structural Modification of MoS_2 Surfaces. *3.1.1. Tribological Behavior of Shear Modified Surfaces Formed in Dry N_2.* The coefficient of friction on cycle 1 for the area previously rastered in dry N_2 was found to be $\mu \sim 0.06$, almost 50% lower than that on the as-deposited region, $\mu \sim 0.12$ (Figure 2a). Not only is the initial friction coefficient reduced, but the subsequent cycles are also slightly lower (Figure 2b) in the rastered area. After 10 sliding cycles the as-deposited and dry N_2 rastered regions have similar steady-state values (Figure 2b).

The initial coating microstructure (Figure 3a) is observed to be composed of randomly oriented nanometer sized crystallites. Sliding in dry N_2 modified the surface microstructure (Figure 3b), forming a thin basally oriented (002) surface layer after 20 sliding cycles. The area rastered in dry N_2, and the as-deposited coating have very different surface microstructures and we show tribological properties are improved with a basally oriented surface microstructure. This improvement, especially in the first cycle of sliding, would be beneficial for applications such as spacecraft deployment mechanisms, that require the lowest possible friction coefficient on the first operation

3.1.2. Tribological Behavior of Shear Modified Surfaces Formed in Air. While the tribological properties of MoS_2 are optimal in inert or vacuum environments, many practical applications require MoS_2 coatings to be operated and stored in the presence of O_2 and H_2O which are known to cause high friction, decreased wear resistance, and oxidation.[30] The coefficient of friction measured during creation of the raster patch in lab air (50% RH) ($\mu \sim 0.2$) was significantly higher than in dry N_2. After forming raster patches in lab air, the rastered region was tribologically tested in dry N_2. The friction loop of the first cycle (Figure 2a) across the raster patch formed in lab air shows that the coefficient of friction is lower ($\mu \sim 0.09$) than the as-deposited region ($\mu \sim 0.12$). The average friction coefficient for the first 10 cycles (Figure 2b) shows that the area rastered in air runs-in to $\mu \sim 0.02$ after just one cycle and thereafter behaves like the as-deposited region.

The difference in tribological behavior between the area rastered in air and the as-deposited coatings could be due to

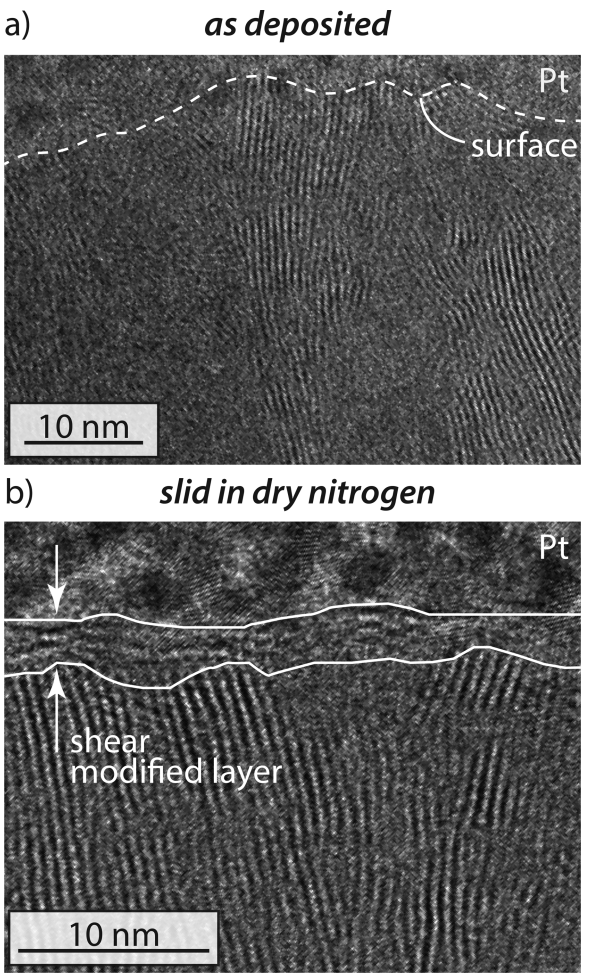

Figure 3. (a) TEM bright-field (BF) image of the as-deposited coating and (b) TEM BF image of the surface after sliding in dry N_2 before aging showing a shear modified layer of basally oriented MoS_2.

shear-induced structural modifications of the surface. While low friction in dry inert environments has been shown to be due to the formation of a low shear strength basally oriented surface, a fundamental understanding of the resulting microstructure for MoS_2 coatings slid in air, and how interactions with air during sliding affects structural changes is lacking. STEM micrographs of the MoS_2 surface slid in lab air show three different shear-induced surface microstructures (Figure 4). While sliding in dry N_2 was shown to form a basally oriented surface (Figure 3b), sliding in lab air can form an amorphous surface (Figure 4 a,d,g) or a basally oriented surface with varying thickness (Figure 4b,c,e,f,h,i).

The surface morphology of the area rastered in air is likely the reason for the different friction behavior than as-deposited MoS_2. Shearing MoS_2 in the presence of O_2 and H_2O structurally alters the surface and impacts the tribological properties. The amorphous surface (Figure 4g) was unexpected and not well understood. One explanation involves the overlapping wear scars in the rastered areas. The wear rate of pure MoS_2 is highest in humid environments, and as individual wear scars are formed, wear debris could be ejected to the edges and then compacted on the surface when the contact is moved to form the next wear scar. Alternatively, shear in the presence of O_2 and H_2O could decrease MoS_2 lamella size through interactions with edge sites and oxidation.

https://doi.org/10.1021/acsami.1c24931
ACS Appl. Mater. Interfaces 2022, 14, 13914−13924

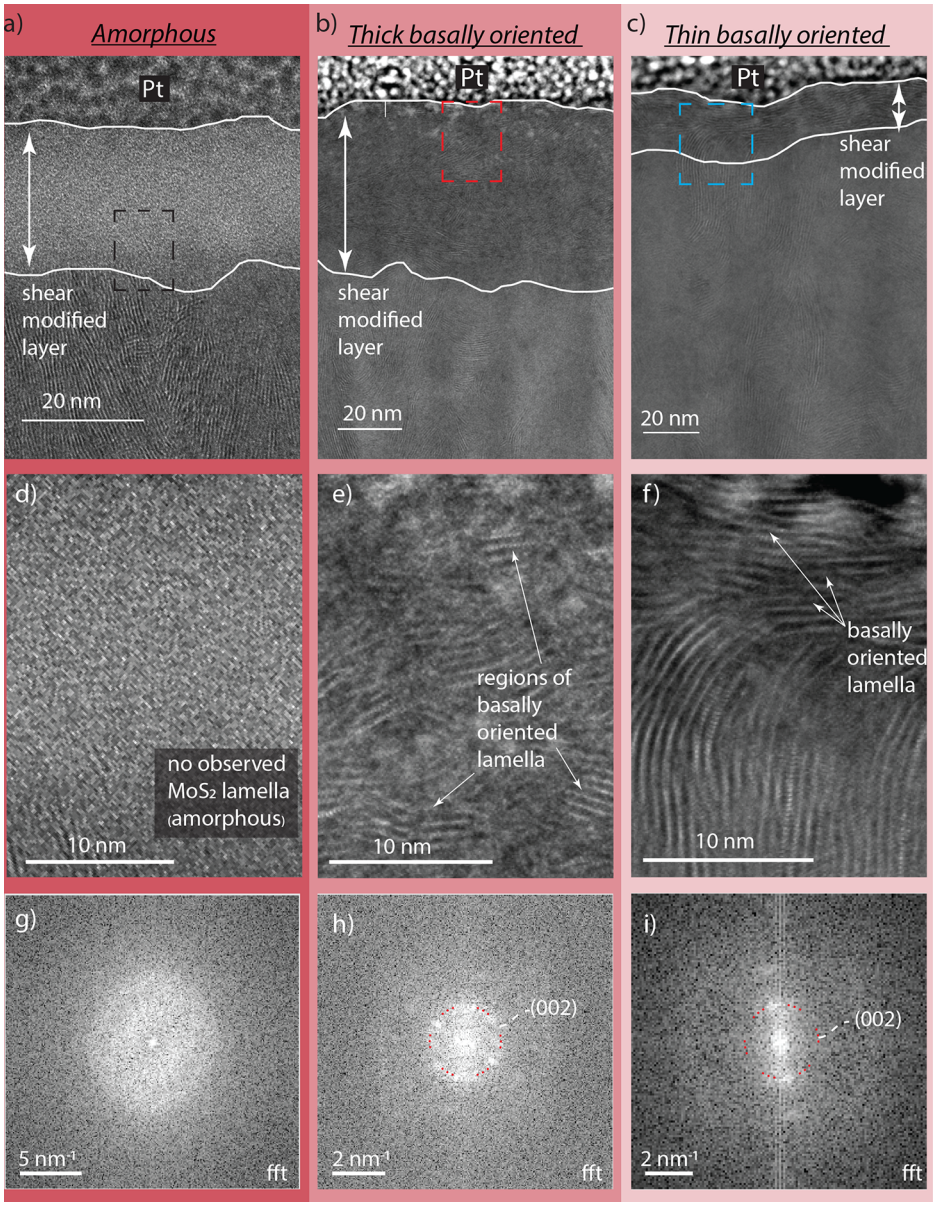

Figure 4. STEM images of three different surface microstructures formed by sliding in lab air: (a) amorphous, (b) thick basally oriented, and (c) thin basally oriented regions. High magnification of each region is shown in (d) amorphous, (e) thick basally oriented, and (f) thin basally oriented. FFT's of each region are shown in (g) amorphous, (h) thick basally oriented, and (i) thin basally oriented.

Previous studies on oxidation and oxidative etching of few-layer MoS_2 by Walter et al.[31] showed that exposure to both H_2O and O_2 decreases the temperature at which MoS_2 is oxidized and increases the rate of oxidative etching. Walter et al. observed that few-layer MoS_2 was etched away from the edges and that the rate of oxidation depends on the number of layers. Kooyman et al. also observed that the particle size and number of layers of supported MoS_2 catalysts start decreasing after 5 min of exposure to air.[37] Additionally, a recent study by Curry et al.[28] showed that H_2O and O_2 passivate edge sites of MoS_2 forming smaller more defective lamella. It is possible that under high contact pressures and shear stresses while exposed to H_2O and O_2 MoS_2 lamella could become amorphous due to a mix of oxidation and passivation of edge sites.

The surface of MoS_2 slid in lab air also exhibited regions that were basally oriented with different thicknesses (Figure 4b,c). Though the friction coefficient of MoS_2 slid in air was high (~0.2), the surface still exhibited shear-induced reorientation (Figure 4h,i) typically associated with low friction. The basally oriented layer ranged from ~50 nm (Figure 4b,e) to ~20 nm (Figure 4c,f) thick, possibly a result of wear or localized changes in contact pressure. While the surface of the lab air raster is composed of both amorphous and basally oriented regions, we expect that the regions of basal orientation will accommodate shear because of having a lower shear strength than the amorphous regions. While it has not been experimentally demonstrated, we imagine that the sliding interface follows the weakest path. A macroscopic contact of steel sliding on an MoS_2-coated steel substrate is dominated by many smaller asperity contacts that when integrated react the normal and friction forces. Increasing the area fraction of basally oriented MoS_2 regions would increase the probability that an asperity carrying a portion of the contact load is instantaneously reacted on a low-shear-strength basally

https://doi.org/10.1021/acsami.1c24931
ACS Appl. Mater. Interfaces 2022, 14, 13914−13924

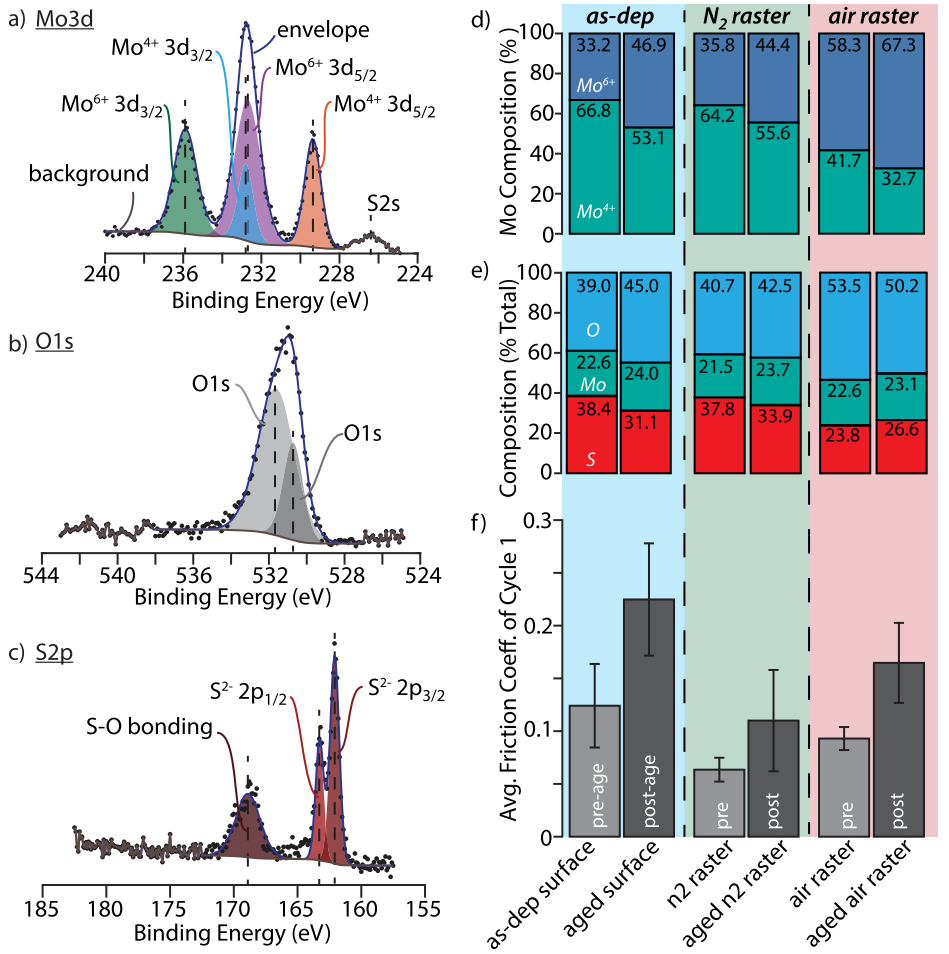

Figure 5. (a–c) Representative XPS spectra (aged air raster) and associated deconvolution showing the (a) Mo 3d region, (b) the O 1s region, and (c) the S 2p region, all with corresponding fits. (d) Mo^{6+} to Mo^{4+} ratio calculated from deconvoluting the XPS Mo 3d photoelectron regions for the as-deposited surface, dry N_2 raster, and lab air raster before and after aging. (e) Derived XPS composition of the as-deposited surface, dry N_2 raster, and lab air raster before and after aging based on Mo 3d, O 1s, and S 2p photoelectron regions. (f) Average friction coefficient of the first sliding cycle for the as-deposited surface, dry N_2 raster, and lab air raster before and after aging.

oriented region, thus reducing the shear strength of the interface. We cannot quantify the ratios of amorphous and basally oriented regions at this time, yet we believe that the low friction coefficient observed in the lab air raster when tested in dry N_2 is a result of an increased percentage of basally oriented MoS_2 in the surface. Curry et al.[28] observed basally oriented MoS_2 after sliding in humid N_2. The TEM micrographs in Figure 4b,c show that reorientation of MoS_2 lamella is possible when sliding in the presence of O_2 and H_2O. Though sliding on the area rastered in air ($\mu \sim 0.09$) and that rastered in dry N_2 ($\mu \sim 0.06$) both showed lower friction than the as-deposited ($\mu \sim 0.12$) area (Figure 2a,b), the coefficient of friction of the area rastered in air was slightly higher than the one rastered in dry N_2 even though both surfaces are basally oriented. As Curry et al. observed in humid N_2,[28] variations in the friction coefficient could be due to varying lamella size defect density caused by the presence of O_2 and H_2O.

These results suggest that preflight testing in lab air is beneficial for decreasing initial friction during subsequent operation when preflight testing in dry N_2 is not achievable or practical.

3.2. Shear-Induced Chemical Modifications of MoS_2 Surfaces. *3.2.1. Composition of Shear Modified MoS_2 in Dry N_2.* XPS was used to probe the surface of the shear modified dry N_2 MoS_2 surface to understand the effects of sliding on the chemical composition. Deconvolution of the Mo 3d, O 1s, and S 2p spectra (Figure 5a–c) was performed to differentiate between MoS_2 (Mo^{4+}) and MoO_3 (Mo^{6+}). The as-deposited surface (Figure 5d) appears to be mostly MoS_2 with some oxide which is expected due to the surface sensitive nature of XPS. XPS of the MoS_2 surface modified by sliding in dry N_2 is comparable to the as-deposited surface with similar amounts of MoS_2 and MoO_3. The composition of the areas rastered in dry N_2 (Figure 5e) and the as-deposited surface are also similar, indicating that sliding in dry N_2 does not significantly change the chemical makeup of MoS_2. While we believe the slight decrease in oxygen from the as-deposited surface to the dry N_2 raster is insignificant, an alternative could be that there is a slight increase in oxygen due to interactions with metal oxides on the steel probe or very mild oxidation due sliding in the presence of low concentrations of water, oxygen (roughly 0.5 ppm for both), and hydrocarbons. The results from XPS support the notion that the decreased friction coefficient observed on the dry N_2 raster cannot be due to chemical changes of the surface but is likely a result of shear induced structural modifications discussed earlier.

3.2.2. Composition of Shear Modified MoS_2 in Air. Areas rastered in lab air were measured with XPS (Figure 5d,e) to

https://doi.org/10.1021/acsami.1c24931
ACS Appl. Mater. Interfaces 2022, 14, 13914–13924

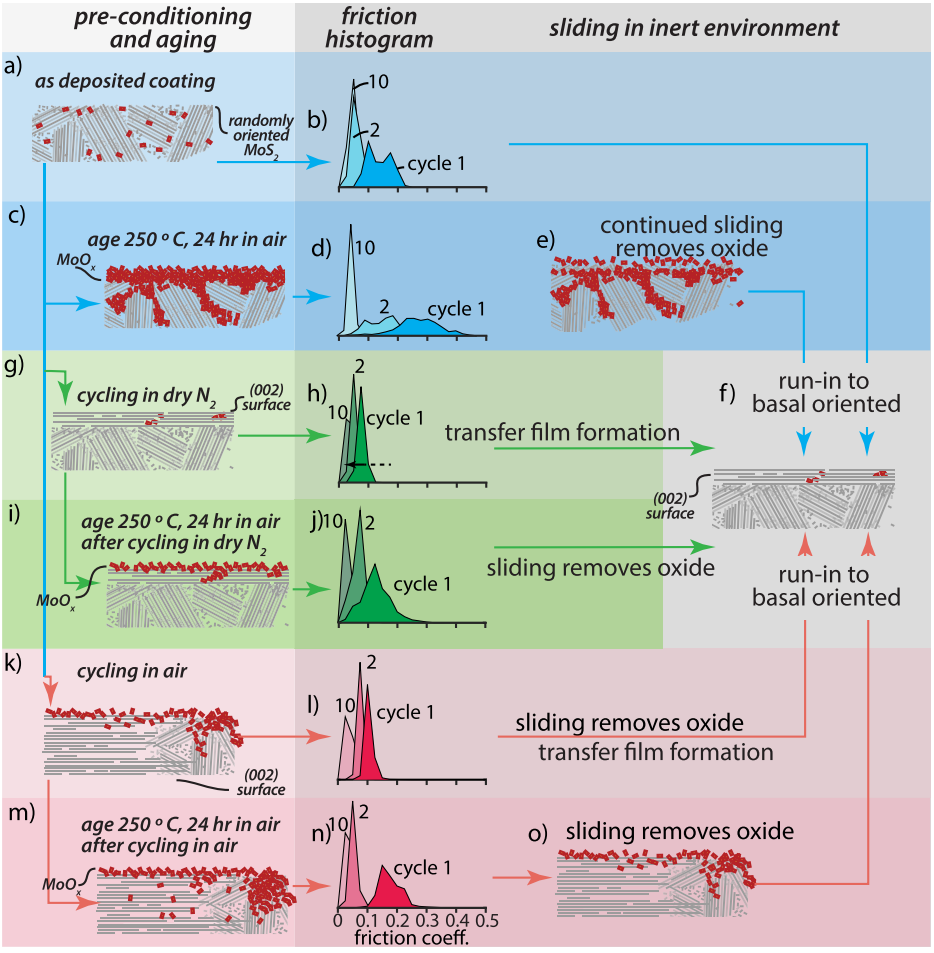

Figure 6. Mechanistic hypothesis describing the oxidation of different MoS_2 surface microstructures. (a) As-deposited MoS_2 coating microstructure and (b) histogram of the first, second, and tenth cycle friction coefficient. (c) Schematic of the aged as-deposited coating showing oxidation of the surface and subsurface with (d) corresponding histograms of measured friction. (e) The process to achieve low friction for an aged as-deposited coating is oxide removal with continuous sliding and eventual low friction after the formation of a (f) basally oriented surface with no oxide. (g) Schematic of the surface microstructure of MoS_2 after sliding in dry N_2 and the histogram of the first, second, and tenth cycles of the raster patch showing the transition to low friction due to transfer film formation (h). (i) Aging of the dry N_2 raster causes mild oxidation of the top surface and maintains good friction behavior as shown in (j). (k) Schematic of the surface microstructure of MoS_2 after being slid in humid lab air showing regions of basal orientation and other nonoriented regions all with mild oxidation. (l) The histograms of friction showing improved friction over the as-deposited coating is due to regions of basal orientation. (m) Aging of the lab air raster slightly increases oxidation of the surface and friction of the first sliding cycle (n), though after a single sliding cycle, (o) oxide is removed and low friction is recovered.

understand how sliding in the presence of water and oxygen impacts the chemical composition of the sliding surface. Analysis of the Mo 3d region from the area rastered in air shows more MoO_3 (Mo^{6+}) and less MoS_2 (Mo^{4+}) than either the area rastered in dry N_2 or the as-deposited coating (Figure 5d). This was confirmed by analysis of the O 1s and S 2p peaks, showing that the area rastered in air contains more oxygen and less sulfur than the as-deposited coating (Figure 5e). One might infer that the friction coefficient of the area rastered in lab air would be highest, but the coefficient of friction of the area rastered in air is lower than that of the as-deposited surface. XPS indicates that sliding in lab air increases the amount of oxygen on the surface, likely a result of oxidation formed during sliding due to interactions between water vapor, oxygen, and MoS_2.[31,38−41] TEM indicates (Figure 4a−c) that the surface is basally oriented (with some amorphous regions). The data suggest that the structural modifications observed by TEM have a larger influence on the tribological properties of MoS_2 than the chemical changes observed by XPS.

3.3. Aging Behavior of Shear Modified MoS_2 Surfaces.

3.3.1. Friction and Oxidation of Shear Modified MoS_2 in Dry N_2. Areas rastered in dry N_2 exhibit very different friction behavior than the as-deposited coating after aging in air (Figure 2c,d). The friction loop of cycle one shows that the coefficient of friction in the rastered area is lower ($\mu \sim 0.11$) than that of the as-deposited coating ($\mu \sim 0.22$). The friction loop shows some regions within the rastered area with a very low ($\mu \sim 0.05$) friction coefficient, almost identical with the preaging case. Additionally, the friction coefficient in the area rastered in dry N_2 and then aged runs in to a low steady state value ($\mu \sim 0.05$) after only one cycle, while the as-deposited coating requires four cycles (Figure 2d). The Mo 3d peak (Figure 5d) exhibits an increase in MoO_3 in the area rastered in dry N_2 and then aged compared to the same area before aging. The as-deposited coating has a similar increase in MoO_3 after aging compared to the area rastered in dry N_2, but the average friction coefficient on cycle one of the rastered area is lower than that on the as-deposited film (Figure 5f).

https://doi.org/10.1021/acsami.1c24931
ACS Appl. Mater. Interfaces 2022, 14, 13914−13924

These results show that the basally oriented surface created by sliding in dry N_2 improves the tribological properties by minimizing surface oxidation and blocking reactive species from penetrating into the coating, in a way similar to coatings initially deposited with basally oriented microstructures.[29] Shear-oriented MoS_2 is expected to have fewer available sites for O_2 and H_2O to adsorb and react than amorphous or nanocrystalline microstructures. Even though the friction coefficient of the area rastered in dry N_2 is lower than that of the as-deposited coating after aging, the two surfaces are chemically similar. The area rastered in dry N_2 showed a smaller increase (~9%) in oxide than the as-deposited surface (~13%) after aging, attributed to the limited oxidation of basally oriented surfaces compared to other structures.

A mechanistic hypothesis describing the oxidation of different MoS_2 surface microstructures is shown in Figure 6. Prior to sliding (i.e., as-deposited coatings, Figure 6a), the friction behavior is typical for pure fresh MoS_2 (Figure 6b). Aging of the as-deposited microstructure causes oxidation of the surface and penetration of oxygen into the coating (Figure 6c), resulting in increased initial friction (cycle 1) and requiring more cycles to run in to low steady-state friction (Figure 6d). Continuous sliding removes surface oxide (Figure 6e), but because of increased oxidation below the surface, multiple sliding passes are required until the formation of a well-oriented basal surface and low steady-state friction is achieved (Figure 6f). The relationship between surface oxide and friction coefficient has been observed by Khare and Burris,[38] who demonstrated that sliding removes surface oxide and that the coefficient of friction decreases as oxide is removed with multiple sliding passes. In our study, the oxide was likely removed in a single cycle, though the amount of sliding cycles required could vary depending on the severity of oxidation and degree to which oxide penetrates the coating.

A second possible route for a MoS_2-coated component/part is cycling in a dry inert environment (Figure 6g). As was shown in Figure 3b, sliding in dry N_2 forms a thin basally oriented tribofilm which decreases the initial friction coefficient during subsequent sliding (Figure 6h). Aging of the basally oriented surface formed by sliding in dry N_2 causes mild oxidation of the surface but the oriented tribofilm prevents significant oxidation of the surface or penetration into the coating (Figure 6i). The increased resistance to oxidation allows for the initial friction coefficient of the aged tribofilm to be lower than the aged unworn coating (Figure 6j), and after just a single sliding cycle, the aged dry N_2 surface achieves low friction due to a basally oriented surface without any oxide (Figure 6f). The results from this study on the aged dry N_2 surface agree well with the observations of Curry et al.[42] on oxidized basally oriented nitrogen sprayed pure MoS_2 coatings. Coatings made by nitrogen spray are basally oriented throughout with large crystallites, while a basally oriented tribofilm created by sliding on a sputtered randomly oriented nanocrystalline coating for only 20 cycles provides similar protection from oxidation and improved friction behavior.

3.3.2. Friction and Oxidation of Shear Modified MoS_2 in Air. MoS_2 surfaces modified by sliding in lab air were subsequently aged and tested in dry N_2 by sliding across the aged raster patches (Figure 2c,d). The friction loop of cycle one (Figure 2c) shows two distinct regions post aging: a higher friction region outside the rastered area and lower friction inside the area rastered in air after aging. While the first cycle friction coefficient of the area rastered in air then aged is lower than the as-deposited coating after aging, it is slightly higher than the coating rastered in dry N_2 and aged. Average friction for the first ten cycles (Figure 2d) of the area rastered in air then aged shows that the surface recovers low friction (<0.05) after one sliding cycle, similar to the area rastered in dry N_2 and aged. The Mo 3d peak (Figure 5d,e) shows that the amount of Mo^{6+} increased from the preaged surface and was the highest for the three tested surfaces. Surprisingly, the S 2p peak (Figure 5e) shows that the area rastered in air and then aged contains slightly more sulfur and less oxygen than prior to aging. While the overall oxygen is lower after aging for the air raster, there is an increase in Mo^{6+} likely associated with MoO_x. The decrease in oxygen composition could come from the loss other oxygen species such SO_x or adsorbed hydrocarbons from the high-temperature aging.[43]

The XPS and tribological experiments indicate that the surface with the most oxide is lower friction than the aged as deposited surface which has ~20% less Mo^{6+}. TEM of the lab air track showed three different structurally modified surface microstructures which impact the tribological properties both pre- and post aging. Basally oriented regions of varying thickness (Figure 4b,c) and amorphous regions (Figure 4a) were formed by sliding in air, yet friction in air is high for MoS_2 (~0.15−0.2). The increased amount of oxide is a result of sliding in air, which, while reorienting MoS_2, partially oxidizes lamella and reincorporates wear debris forming amorphous islands (Figure 6k). The initial friction coefficient of the area rastered in air is still low when tested in dry N_2 (Figure 6i) because the basally oriented regions have a low shear strength. The aging mechanisms for a surface sheared in air (Figure 6m) are very similar to the dry N_2 surface with regions of basally oriented MoS_2 limiting surface oxidation and penetration of oxide into the bulk coating. While the area rastered in dry N_2 is covered by basally oriented MoS_2 lamella, the area rastered in air has small amorphous regions that are less resistant to oxidation which contribute to a higher initial friction coefficient after aging than the aged dry N_2 surface (Figure 6n). After just a single sliding cycle, any effects of aging are removed (Figure 6o), and the area rastered in air then aged returns to low friction (Figure 6f). The initial coefficient of friction of the area rastered in air then aged is dramatically reduced compared to the aged as deposited coating, supporting the notion that preflight testing of MoS_2 coating is important for improving oxidation resistance and tribological properties. While the friction of an area rastered in dry N_2 then aged is slightly lower than an area rastered in air then aged, the practical difficulties of operating every component or system in an inert environment could prove challenging.

3.3.3. Impacts on Applications in Space Tribology. Figure 6 is also helpful for understanding the lifecycles of coatings in a space tribology application. A coating that is not tested or run-in before flight but not exposed to reactive oxygen species will have significantly higher first and early cycle friction (Figure 6b). If a coating is subjected to an oxidative environment without being run-in, the friction will be even higher in early cycles (Figure 6d) due to oxidation of the surface, especially in randomly or columnar oriented sputtered MoS_2 films. Curry et al. showed that this can be minimized with basally oriented coating.[29] Controlling the orientation of MoS_2 microstructure is currently a challenge for sputter deposition techniques.

Sliding on a MoS_2 coating reorients the surface microstructure of otherwise randomly oriented films. In many cases, a design engineer has an obligation to test and validate the

https://doi.org/10.1021/acsami.1c24931
ACS Appl. Mater. Interfaces 2022, 14, 13914−13924

operation of mechanical system and subsystems that have sliding interfaces. The impact of the preflight testing on the in-flight performance has been overlooked in many cases. A challenging decision is balancing the number of test cycles required to validate the component against alterations in the component lifetime due to wear of the solid lubricant of finite thickness. The results presented here show that preflight sliding is acceptable and reduces the first cycle friction in orbit and the effects of oxidation (for example, atomic oxygen in low earth orbit) on the tribological properties.

Our results show that run-in in an inert environment (i.e., dry N_2 or vacuum) provides protection of the surface from oxidative species and significantly lower first cycle friction on orbit. Although preflight testing of components in inert environments is ideal, inherent challenges such as system size, cost, availability, and time associated with environmentally controlled testing may be prohibitive. The alternative of testing in air environments still provides favorable changes to the surface microstructure and can ultimately result in better on-orbit performance and oxidation resistance compared to systems that are never tested before flight.

4. CONCLUSIONS

This work illustrates how sliding in different environments structurally alters the surface of pure MoS_2 coatings and the role that these modified structures have on subsequent friction performance and aging. Sheared areas (raster patches) were created in lab air (~50% RH) and dry N_2. The friction coefficient was measured inside each raster patch before and after aging and compared to the as-deposited coating. Results show that sliding in dry N_2 forms a basally oriented tribofilm which has a lower initial friction coefficient than the as-deposited surface when subsequently slid on. Experiments in lab air showed that sliding in the presence of water and oxygen can structurally alter the surface of MoS_2, resulting in various microstructures ranging from amorphous to basally oriented. The surface created in lab air was shown to have a lower coefficient of friction than the as-deposited coating with fewer cycles to run-in to low friction.

XPS of the raster patch formed in dry N_2 showed no significant change in chemistry compared to the as-deposited coating, indicating that the improved tribological properties of the dry N_2 raster are a result of the basally ordered surface. XPS of the lab air raster found that the surface was more oxidized than the as-deposited coating, yet the tribological properties were improved. This suggests that the chemical degradation of the surface MoS_2 has a smaller impact on tribological properties than the MoS_2 microstructure. Dry N_2 and lab air raster patches were aged at 250 °C for 24 h. The results showed that the aged as-deposited coating exhibited a significant increase in friction, while prior sliding in both dry N_2 and lab air minimized the effects of aging. XPS showed that the aged dry N_2 surface was very similar to the aged as-deposited surface with a slight increase in Mo^{6+} (indicating oxidation), while the aged lab air raster had the most Mo^{6+}.

This work demonstrates that testing a component coated with MoS_2 in inert or lab air environments structurally alter the surface, allowing for improved tribological properties and resistance to oxidation from aging. The utility of this work for space applications highlights the importance of preflight testing. However, a question remains regarding the number of preflight cycles required to impart this benefit and how to balance this against the effects of wear.

AUTHOR INFORMATION

Corresponding Author

Brandon A. Krick − *FAMU-FSU College of Engineering, Florida State University, Tallahassee, Florida 32310, United States;* orcid.org/0000-0003-3191-5433; Email: bkrick@fsu.edu

Authors

Tomas F. Babuska − *FAMU-FSU College of Engineering, Florida State University, Tallahassee, Florida 32310, United States; Material, Physical and Chemical Sciences Center, Sandia National Laboratories, Albuquerque, New Mexico 87123, United States; Mechanical Engineering Department, Lehigh University, Bethlehem, Pennsylvania 18015, United States*

John F. Curry − *Material, Physical and Chemical Sciences Center, Sandia National Laboratories, Albuquerque, New Mexico 87123, United States*

Michael T. Dugger − *Material, Physical and Chemical Sciences Center, Sandia National Laboratories, Albuquerque, New Mexico 87123, United States*

Ping Lu − *Material, Physical and Chemical Sciences Center, Sandia National Laboratories, Albuquerque, New Mexico 87123, United States*

Yan Xin − *National High Magnetic Field Laboratory, Florida State University, Tallahassee, Florida 32310, United States*

Sam Klueter − *Department of Materials Science and Engineering, University of Maryland, College Park, Maryland 20742, United States*

Alexander C. Kozen − *Department of Materials Science and Engineering, University of Maryland, College Park, Maryland 20742, United States*

Tomas Grejtak − *FAMU-FSU College of Engineering, Florida State University, Tallahassee, Florida 32310, United States; Mechanical Engineering Department, Lehigh University, Bethlehem, Pennsylvania 18015, United States*

Complete contact information is available at: https://pubs.acs.org/10.1021/acsami.1c24931

Notes

The authors declare no competing financial interest.

ACKNOWLEDGMENTS

This material is based upon work supported by the National Science Foundation under Grant 2027029, Grant 1826251, and NSF GRFP 1842163. TEM work was performed at the National High Magnetic Field Laboratory, which is supported by National Science Foundation Cooperative Agreement DMR-1644779 and the State of Florida. This work was funded by the Laboratory Directed Research and Development (LDRD) program at Sandia National Laboratories, a multi-mission laboratory managed and operated by National Technology and Engineering Solutions of Sandia, LLC, a wholly owned subsidiary of Honeywell International, Inc., for the U.S. Department of Energy's National Nuclear Security Administration under Contract DE-NA0003525. This paper describes objective technical results and analysis. Any subjective views or opinions that might be expressed in the paper do not necessarily represent the views of the U.S. Department of Energy or the United States Government.

https://doi.org/10.1021/acsami.1c24931
ACS Appl. Mater. Interfaces 2022, 14, 13914−13924

REFERENCES

(1) Hilton, M. R.; Fleischauer, P. D. Applications of Solid Lubricant Films in Spacecraft. *Surf. Coat. Technol.* **1992**, *54*−*55*, 435−441.
(2) Donnet, C.; Martin, J. M.; le Mogne, T.; Belin, M. Super-Low Friction of MoS_2 Coatings in Various Environments. *Tribiol. Int.* **1996**, *29* (2), 123−128.
(3) Roberts, E. W. Ultralow Friction Films of MoS_2 for Space Applications. *Thin Solid Films* **1989**, *181* (1−2), 461−473.
(4) Fayeulle, S.; Ehni, P. D.; Singer, I. L. Paper V (II) Role of Transfer Films in Wear of MoS_2 Coatings. *Tribology Series* **1990**, *17* (C), 129−138.
(5) Fleischauer, P. D.; Bauer, R. Chemical and Structural Effects on the Lubrication Properties of Sputtered MoS2 Films. *Tribiol. Trans.* **1988**, *31* (2), 239−250.
(6) Holinski, R.; Gänsheimer, J. A Study of the Lubricating Mechanism of Molybdenum Disulfide. *Wear* **1972**, *19* (3), 329−342.
(7) Oviedo, J. P.; Kc, S.; Lu, N.; Wang, J.; Cho, K.; Wallace, R. M.; Kim, M. J. In Situ TEM Characterization of Shear-Stress-Induced Interlayer Sliding in the Cross Section View of Molybdenum Disulfide. *ACS Nano* **2015**, *9* (2), 1543−1551.
(8) Hu, J. J.; Wheeler, R.; Zabinski, J. S.; Shade, P. A.; Shiveley, A.; Voevodin, A. A. Transmission Electron Microscopy Analysis of Mo-W-S-Se Film Sliding Contact Obtained by Using Focused Ion Beam Microscope and in Situ Microtribometer. *Tribol. Lett.* **2008**, *32* (1), 49−57.
(9) Martin, J. M.; Pascal, H.; Donnet, C.; le Mogne, T.; Loubet, J. L.; Epicier, T. Superlubricity of MoS_2: Crystal Orientation Mechanisms. *Surf. Coat. Technol.* **1994**, *68*−*69* (C), 427−432.
(10) Hoffman, E. E.; Marks, L. D. Soft Interface Fracture Transfer in Nanoscale MoS_2. *Tribol. Lett.* **2016**, *64* (1), 1−10.
(11) Pritchard, C.; Midgley, J. W. The Effect of Humidity on the Friction and Life of Unbonded Molybdenum Disulphide Films. *Wear* **1969**, *13* (1), 39−50.
(12) Gardos, M. N. Anomalous Wear Behavior of MoS_2 Films in Moderate Vacuum and Dry Nitrogen. *Tribol. Lett.* **1995**, *1* (1), 67−85.
(13) Vierneusel, B.; Schneider, T.; Tremmel, S.; Wartzack, S.; Gradt, T. Humidity Resistant MoS_2 Coatings Deposited by Unbalanced Magnetron Sputtering. *Surf. Coat. Technol.* **2013**, *235*, 97−107.
(14) Buck, V. Preparation and Properties of Different Types of Sputtered MoS_2 Films. *Wear* **1987**, *114* (3), 263−274.
(15) Fleischauer, P. D. Effects of Crystallite Orientation on Environmental Stability and Lubrication Properties of Sputtered MoS. *ASLE Transactions* **1984**, *27* (1), 82−88.
(16) Fleischauer, P. D. Fundamental Aspects of the Electronic Structure, Materials Properties and Lubrication Performance of Sputtered MoS_2 Films. *Thin Solid Films* **1987**, *154* (1−2), 309−322.
(17) Lince, J. R.; Fleischauer, P. D. Crystallinity of Rf-Sputtered MoS_2 Films. *J. Mater. Res.* **1987**, *2* (6), 827−838.
(18) Fleischauer, P. D.; Lince, J. R. Comparison of Oxidation and Oxygen Substitution in MoS_2 Solid Film Lubricants. *Tribiol. Int.* **1999**, *32* (11), 627−636.
(19) Lince, J. R. $MoS_{2-X}O_x$ Solid Solutions in Thin Films Produced by Rf- Sputter- Deposition. *J. Mater. Res.* **1990**, *5* (1), 218−222.
(20) Muratore, C.; Voevodin, A. A. Chameleon Coatings: Adaptive Surfaces to Reduce Friction and Wear in Extreme Environments, 2009.
(21) Scharf, T. W.; Kotula, P. G.; Prasad, S. v. Friction and Wear Mechanisms in MoS_2/Sb_2O_2 /Au Nanocomposite Coatings. *Acta Mater.* **2010**, *58* (12), 4100−4109.
(22) Centers, P. W. Tribological Performance of MoS2 Compacts Containing MoO_3, Sb_2O_3 or MoO_3 and Sb_2O_3. *Wear* **1988**, *122* (1), 97−102.
(23) Zabinski, J. S.; Bultman, J. E.; Sanders, J. H.; Hu, J. J. Multi-Environmental Lubrication Performance and Lubrication Mechanism of MoS_2/Sb_2O_3/C Composite Films. *Tribol. Lett.* **2006**, *23* (2), 155−163.
(24) Lince, J. R. Tribology of Co-Sputtered Nanocomposite Au/MoS_2 Solid Lubricant Films over a Wide Contact Stress Range. *Tribol. Lett.* **2004**, *17* (3), 419−428.
(25) Spalvins, T. Frictional and Morphological Properties of Au-MoS_2 Films Sputtered from a Compact Target. *Thin Solid Films* **1984**, *118* (3), 375−384.
(26) Hilton, M. R.; Bauer, R.; Didziulis, S. v.; Dugger, M. T.; Keem, J. M.; Scholhamer, J. Structural and Tribological Studies of MoS_2 Solid Lubricant Films Having Tailored Metal-Multilayer Nanostructures. *Surf. Coat. Technol.* **1992**, *53* (1), 13−23.
(27) Curry, J. F.; Argibay, N.; Babuska, T.; Nation, B.; Martini, A.; Strandwitz, N. C.; Dugger, M. T.; Krick, B. A. Highly Oriented MoS_2 Coatings: Tribology and Environmental Stability. *Tribol. Lett.* **2016**, *64* (1), 1−9.
(28) Curry, J. F.; Ohta, T.; DelRio, F. W.; Mantos, P.; Jones, M. R.; Babuska, T. F.; Bobbitt, N. S.; Argibay, N.; Krick, B. A.; Dugger, M. T.; Chandross, M. Structurally Driven Environmental Degradation of Friction in MoS_2 Films. *Tribology Letters* **2021**, *69* (3), 1−10.
(29) Curry, J. F.; Wilson, M. A.; Luftman, H. S.; Strandwitz, N. C.; Argibay, N.; Chandross, M.; Sidebottom, M. A.; Krick, B. A. Impact of Microstructure on MoS_2 Oxidation and Friction. *ACS Appl. Mater. Interfaces* **2017**, *9* (33), 28019−28026.
(30) Lince, J. R.; Loewenthal, S. H.; Clark, C. S. Tribological and Chemical Effects of Long Term Humid Air Exposure on Sputter-Deposited Nanocomposite MoS_2 Coatings. *Wear* **2019**, *432-433*, 202935.
(31) Walter, T. N.; Kwok, F.; Simchi, H.; Aldosari, H. M.; Mohney, S. E. Oxidation and Oxidative Vapor-Phase Etching of Few-Layer MoS_2. *Journal of Vacuum Science & Technology B, Nanotechnology and Microelectronics: Materials, Processing, Measurement, and Phenomena* **2017**, *35* (2), No. 021203.
(32) Gao, J.; Li, B.; Tan, J.; Chow, P.; Lu, T.-M.; Koratkar, N. Aging of Transition Metal Dichalcogenide Monolayers. *ACS Nano* **2016**, *10* (2), 2628−2635.
(33) Gosvami, N. N.; Bares, J. A.; Mangolini, F.; Konicek, A. R.; Yablon, D. G.; Carpick, R. W. Tribology. Mechanisms of Antiwear Tribofilm Growth Revealed in Situ by Single-Asperity Sliding Contacts. *Science (New York, N. Y.)* **2015**, *348* (6230), 102−106.
(34) Krick, B. A.; Vail, J. R.; Persson, B. N. J.; Sawyer, W. G. Optical in Situ Micro Tribometer for Analysis of Real Contact Area for Contact Mechanics, Adhesion, and Sliding Experiments. *Tribol. Lett.* **2012**, *45* (1), 185−194.
(35) Colbert, R. S.; Krick, B. A.; Dunn, A. C.; Vail, J. R.; Argibay, N.; Sawyer, W. G. Uncertainty in Pin-on-Disk Wear Volume Measurements Using Surface Scanning Techniques. *Tribology Letters 2011 42:1* **2011**, *42* (1), 129−131.
(36) Burris, D. L.; Sawyer, W. G. Addressing Practical Challenges of Low Friction Coefficient Measurements. *Tribology Letters 2009 35:1* **2009**, *35* (1), 17−23.
(37) Kooyman, P. J.; Rob van Veen, J. A. The Detrimental Effect of Exposure to Air on Supported MoS_2. *Catal. Today* **2008**, *130* (1), 135−138.
(38) Khare, H. S.; Burris, D. L. Surface and Subsurface Contributions of Oxidation and Moisture to Room Temperature Friction of Molybdenum Disulfide. *Tribol. Lett.* **2014**, *53* (1), 329−336.
(39) Atkinson, I. B.; Swift, P. A Study of the Tribo-Chemical Oxidation of Molybdenum Disulphide Using X-Ray Photo-Electron Spectroscopy. *Wear* **1974**, *29* (1), 129−133.
(40) Spychalski, W. L.; Pisarek, M.; Szoszkiewicz, R. Microscale Insight into Oxidation of Single MoS_2 Crystals in Air. *J. Phys. Chem. C* **2017**, *121* (46), 26027−26033.
(41) Ross, S.; Sussman, A. Surface Oxidation of Molybdenum Disulfide. *J. Phys. Chem.* **1955**, *59* (9), 889−892.
(42) Curry, J. F.; Wilson, M. A.; Luftman, H. S.; Strandwitz, N. C.; Argibay, N.; Chandross, M.; Sidebottom, M. A.; Krick, B. A. Impact of Microstructure on MoS_2 Oxidation and Friction. *ACS Appl. Mater. Interfaces* **2017**, *9* (33), 28019−28026.

https://doi.org/10.1021/acsami.1c24931
ACS Appl. Mater. Interfaces 2022, 14, 13914−13924

(43) Afanasiev, P.; Lorentz, C. Oxidation of Nanodispersed MoS_2 in Ambient Air: The Products and the Mechanistic Steps. *J. Phys. Chem. C* **2019**, *123* (12), 7486−7494.

https://doi.org/10.1021/acsami.1c24931
ACS Appl. Mater. Interfaces 2022, 14, 13914−13924